Technical Note

Influence of Ultrasound Settings on Laboratory Vertical Artifacts

Joao Leote [a,b,*], Tiago Muxagata [b], Diana Guerreiro [b], Cláudia Francisco [b], Hermínia Dias [b], Ricardo Loução [c], Jacobo Bacariza [a], Filipe Gonzalez [a], on behalf of the EchoCrit Group [a]

[a] Critical Care Department, Hospital Garcia de Orta EPE, Almada, Portugal
[b] Escola Superior de Tecnologia da Saúde de Lisboa, Instituto Politécnico de Lisboa, Lisboa, Portugal
[c] Center of Neurosurgery, University Hospital of Cologne, Cologne, Germany

ARTICLE INFO	
Keywords: Lung ultrasound Vertical artifacts Ultrasound Settings B-lines	*Objective:* The aim of the work described here was to analyze the relationship between the change in ultrasound (US) settings and the vertical artifacts' number, visual rating and signal intensity *Methods:* An *in vitro* phantom consisting of a damp sponge and gelatin mix was created to simulate vertical artifacts. Furthermore, several US parameters were changed sequentially (*i.e.,* frequency, dynamic range, line density, gain, power and image enhancement) and after image acquisition. Five US experts rated the artifacts for number and quality. In addition, a vertical artifact visual score was created to determine the higher artifact rating ("optimal") and the lower artifact rating ("suboptimal"). Comparisons were made between the tested US parameters and baseline recordings. *Results:* The expert intraclass correlation coefficient for the number of vertical artifacts was 0.694. The parameters had little effect on the "optimal" vertical artifacts but changed their number. Dynamic range increased the number of discernible vertical artifacts to 3 from 36 to 102 dB. *Conclusion:* The intensity did not correlate with the visual rating score. Most of the available US parameters did not influence vertical artifacts.

Introduction

Lung ultrasound (LUS) is a validated tool for diagnosing and following up lung diseases [1−4]. LUS insonates the thorax between the ribs to obtain images of the pleura and lung, and the evaluation is based on artifacts [5], with vertical artifacts being one of them [6,7]. Vertical artifacts were first observed when subpleural interlobular septa surrounded by subpleural air-filled alveoli become edematous [7,8]. Soldati et al. [9] later introduced the term *acoustic trap* in the generation of vertical artifacts, including B-lines. Demi and colleagues [9−12] clarified the influence of ultrasound (US) waves within lung tissue volumes, with reduced aeration forming such acoustic traps and leading to vertical artifacts, whereas Mohanty et al. [13] illustrated the potential methods to quantify the scattering of US waves in rat lungs. In a healthy lung, vertical artifacts may be present in one or two lung regions, predominantly in the lower lobes [14,15], but the presence of three or more vertical artifacts in two or more lung regions has diagnostic value in pulmonary edema and interstitial diseases [14,15−17]. The absence of vertical artifacts also has a positive predictive value of 91% for a pulmonary artery occlusion pressure below 13 mm Hg [18]. Furthermore, their number is strongly correlated ($r^2 = 0.88$) with an extravascular lung water index estimated by invasive hemodynamic monitoring techniques, guiding fluid resuscitation in critically ill patients [19].

Vertical artifact recording, however, is an operator- and hardware-dependent technique [16,20,21] influenced by several factors such as type of probe, probe orientation and US settings [16,21,22]. Recently, an LUS consensus and guidelines article was published, stating some differences regarding the previous guidelines, published in 2012 [5]. In the consensus of 2012 [5], the vertical artifacts were referred to as B-lines, defined as discrete laser-like vertical hyperechoic reverberation artifacts arising from the pleural line, extending to the bottom of the screen without fading and moving synchronously with lung sliding. Although, considering the recent findings on the "acoustic trap" theory, the recent consensus [23] states that vertical artifacts originate from US wave scatters formed in the acoustic traps, and their appearance differs depending on the subpleural pathophysiology, the US pulse center frequency, bandwidth and shape of the probe. Because of B-line variability when changing US parameters such as frequency, the term *vertical artifacts* has been preferred to *B-lines* in recent studies [11,12,21,24,25] and is used throughout this article.

For this reason, non-optimized US settings may alter the morphology and number of vertical artifacts. Regarding the types of probes, linear transducers produce less intense vertical artifacts [21,25,26]. Moreover, probe size and frequency range may be relevant in the pediatric population [27]. Microconvex and linear transducers are conventionally placed parallel to the pleura without requiring much depth because of lung size [27]. Regarding morphology, the width of the vertical artifact increases

---

J. Leote et al.

when the US focus is placed deeper in the lung tissue and the probe is parallel to the pleura (*i.e.,* incidence angle of 0°), whereas high probe frequency, tissue harmonic imaging and a 0° probe angle attenuate the echogenicity of the vertical artifact mainly in the deeper regions [26,28]. Spatial compound imaging increases the number of vertical artifacts radiating from the same pleura point [29]. Decreased dynamic range (<45 dB), absence of a focal zone and imaging harmonics, frame averaging and high dynamic range are known to worsen *in vitro* vertical artifacts significantly [30]. In fact, the focal zone at the level of the pleura, absence of harmonics and linear time gain to far-field increased visual rating and vertical artifact quantity when using a curvilinear probe [29]. Mento and colleagues [28,31] also determined that vertical artifacts were significantly affected by the center frequency, focal point bandwidth and angle of incidence (*i.e.,* type of probe). In fact, these findings were incorporated into the new consensus [23]. Therefore, the observed vertical artifacts are affected not only by the proportion of water or air in the alveoli, but also by the wide variety of parameters provided by US machines. In addition, the influence of these parameters on vertical artifacts was not tested systematically *in vitro* using a visual (and subjective) approach as used in clinical practice. The present study was aimed at comprehensively analyzing the effects of US imaging parameters on the number, visual rating and signal intensity of vertical artifacts produced experimentally in an *in vitro* model.

Methods

The present study was quasi-experimental. An *in vitro* model was devised to simulate subcutaneous tissue, pleura, and the air-lung interface to generate vertical artifacts. Phantom vertical artifacts were accepted if presented as originating from the pleural line, blurring pleura reverberation artifacts, exhibiting a well-defined border contrast and extending deeper to the bottom of the US image.

Vertical artifacts have also been described to move with respiration [5]. However, this phantom did not simulate respiration, and thus, no movement of the artifacts could be assessed. Despite the lack of this feature, in this *in vitro* study, we considered the observed artifacts to resemble the vertical artifacts we aimed for.

In vitro *model*

The *in vitro* model was created to simulate the probable physical origin of the vertical artifacts, that is, aerated alveoli wall reflection of trapped energy [23]. Four phantoms were created with a superficial layer to simulate subcutaneous fat and a deep layer to simulate lung tissue with water in the alveoli. The superficial layer consisted of a mixture of gelatin and sugar-free Metamucil with a ratio of 3:1 per liter of water to recreate the subcutaneous tissue [32]. A solution was created from half a liter of boiling distilled water with 85 g of Condi sugar-free neutral gelatin, stirred until dissolved. After that, while the solution was still warm, 28 g of Metamucil was added and stirred until it was dissolved. The solution was poured into a plastic container and placed in the refrigerator until it became solid [33]. The deeper layer was a damp sponge placed beneath the gelatin. This sponge had 270 μm-mean-diameter pores with a standard deviation (SD) of 130 μm spaced by about 10 μm septa, evaluated through electron microscopy (Fig. 1A). Additionally, a plastic film was placed between the two to simulate the pleura. Overall, a 6-cm deep phantom was constructed, with 3 cm below the "pleural line."

Experimental setup and imaging acquisition

To record images without the influence of probe position and movement, a holder was created to ensure stable and immobile evaluation. This support consisted of a 10-cm high metal base with a flexible aluminum arm at the top to hold the probe (Fig. 1B). The probe's position was marked in three dimensions using a built-in smartphone gyroscope

(Huawei p40 pro, Huawei Technologies Co., Inc., Shenzhen, China) inserted into the probe holder parallel to the probe with the Physics Toolbox application (Vieyra Software).

For US image acquisition, we selected a microcurvilinear probe with a 20-mm radius, field of view of 104°, frequency range between 4 and 8 Hz and 64 piezoelectric elements (code MC8-4R20S-3, Telemed, Vilnius, Lithuania). This probe was part of a portable US system that included a tablet (Surface Pro 7, Microsoft, Redmond, WA, USA) and a MicroUS-EXT H1 beamformer (Telemed). The beamformer was equipped with an AD843 amplifier, which acquires US signal from 192 channels with a 34 MHz bandwidth sampling frequency and 135 ns of settling time. A frame rate of up to 120 Hz was used. After amplification of the signal and its conversion to digital (8 bits), spatial filtering (2-D 16×16 kernel Gaussian filter) of each frame and temporal filtering of two consecutive frames were applied to reduce noise and speckle and enhance edges. No other pre-processing imaging or tissue equalization techniques were used. Time gain compensation was the same across the phantom's depth.

The probe was placed in the holder, in contact with the phantom, with enough gel to obtain a good US image (Fig. 1B). The probe's angulation in relation to the phantom was selected after obtaining an image with well-defined vertical artifacts; once this position was found, the image was acquired after recording gyroscope coordinates. Image acquisition was accomplished by placing a single focus marker on the "pleural line" and using the US settings based on system vendor, current guidelines and literature reports [16,23,34]. US images were recorded with the following US parameters: mechanical index of 0.3, power of −10 dB, gain of 75%, frequency of 4 MHz, medium line density, dynamic range (DR) of 60 dB, and without artifact rejection, image enhancement, speckle reduction or frame averaging (FA). These settings were considered the baseline recordings. Test recordings were acquired after varying a set of selected parameters within proportional steps of available levels in each of the aforementioned parameters. A total of 25 combinations were evaluated per phantom (Table S1, online only).

DICOM 3-s clips were recorded, but the first 30 frames of each clip were excluded to ensure stable performance of the probe. Each US clip was recorded after varying only one of the settings. US acquisition for each phantom was performed immediately after wetting the sponge and within a maximum of 20 min. Gyroscope data and imaging recording were done without probe movements.

Vertical artifact score and intensity

To ensure their adequate clinical similarity, the vertical artifacts were validated by a five-member expert panel (author EchoCrit Group), with 3 to 10 y of experience in LUS. Furthermore, a descriptive feature scale was created to assess the vertical artifact morphology. In Figure 1C is an example obtained from a vertical artifact in a healthy participant to facilitate further interpretation. The created vertical artifact score consisted of a scale from 4 to 12 points, where 4 represented the worst possible vertical artifacts and 12 the best possible artifacts. The score included the pleura classification as regular (1 point), irregular (3 points) or blurred (2 point). The same rationale was applied to the homogeneity of the vertical artifact. The clearness of the horizontal border between the vertical artifact and surrounding medium was classified as well defined (3 points), blurred (2 points) or undefined (1 point). Regarding the length of the vertical artifact, points were awarded according to the following artifact lengths, measured from the pleural line: 1 point if between 0 and 10 mm; 2 points if between 10 and 20 mm; and 3 points if greater than 20 mm.

The panel of US experts was asked to number and score each of the observable artifacts in the US baseline recordings. For an acceptable US image phantom, three or more vertical artifacts and a well-defined pleura had to be present. Then, experts were asked to quantify the number of vertical artifacts and to score the artifacts in test recordings. For comparative purposes, the vertical artifact with the highest average
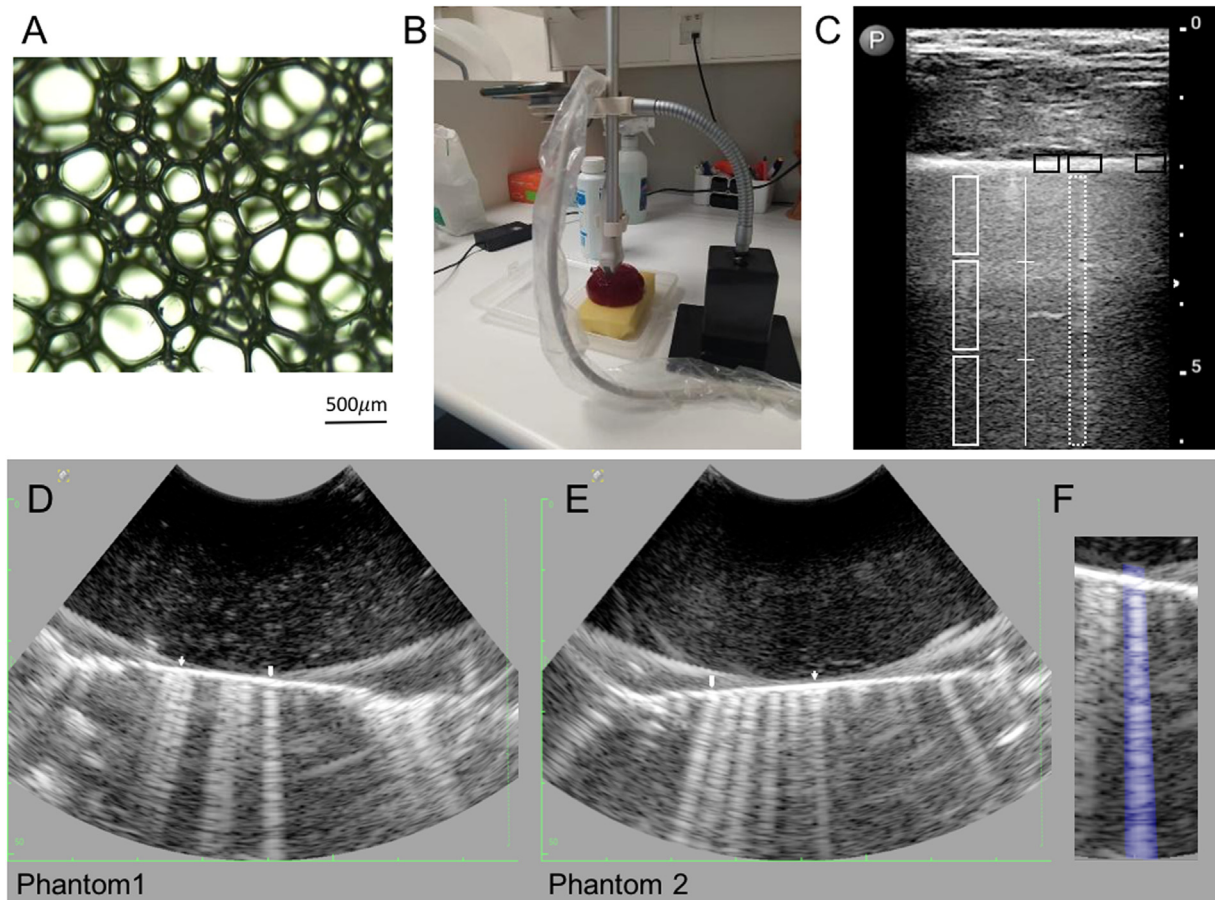
Figure 1. (A, B) The *in vitro* model was based in a sponge (A) with a mean pore diameter of 270 μm, placed below a gelatin/metamucil mixture (B). The probe was placed above the model, and 3-D movement was avoided after it was mounted in a homemade structure. (C) The vertical artifact score included the pleura (*black squares*) from regular (1 point), irregular (3 points) and blurred (left to right). The length of the vertical artifact (*white line*) was awarded 1 point if it was between 0 and 10 mm, 2 points if between 10 and 20 mm or 3 points if spanning further than 20 mm beyond the pleural line. The same rationale was applied for the homogeneity of the vertical artifact (*white rectangle*). The horizontal border between the vertical artifact and surrounding medium (*dashed rectangle*) was well-defined (3 points), blurred (2 points) or undefined (1 point). (D, E) An ultrasound frame of each phantom featuring the optimal (*head arrow*) and suboptimal (*arrow*) artifacts. The lateral parts of the models with irregular "pleura" were ignored. (F) Example of the selected region of interest.

score among all panel members was referred to as the "optimal" and the artifact with the lowest score but still resembling a clinical vertical artifact was referred to as the "suboptimal" (Fig. 1D, 1E).

The imaging analysis was also performed after importing the DICOM clips to an in-house computer (4GB RAM MacBook, Apple Inc, Cupertino, CA, USA). Signal intensity was extracted from the optimal and suboptimal vertical artifacts using an analysis algorithm described in the literature (Mento and Demi [28], implemented in MATLAB (The MathWorks, Natick, MA, USA). The signal intensity (in dB) was calculated having as reference value the maximum signal amplitude from a region of interest (ROI). These ROIs were manually drawn, such that they included either the optimal or suboptimal artifacts, spanning from the pleural line to the bottom of the image (Fig. 1F). The same selected region was used in all the US clips (baseline vs. test recordings).

Data statistical analysis

Imaging data were described as either categorical variables, summarized as counts, or continuous variables. The continuous variables were compared using an independent *t*-test. Correlations for dichotomous and categorical variables were tested with the Spearman correlation. Intraclass correlation coefficient estimates and their 95% confidence intervals were also calculated based on a mean-rating ($k = 5$), absolute-agreement, two-way mixed-effects model. Before performing the statistical tests, we ensured that the extracted data met all required assumptions.

Statistical analyses were performed using SPSS Statistics, version 24 (IBM, Armonk, NY, USA). A *p* value <0.05 was considered to indicate statistical significance.

Results

All phantoms created exhibited vertical artifacts, but the LUS expert panel selected two phantoms (Fig. 1D, 1E) because of closer resemblance to the vertical artifacts observed in clinical practice. The averaged intraclass correlation coefficient for the number of vertical artifacts was 0.694 (95% confidence interval: 0.52−0.87). Table 1 outlines the mean values for number of vertical artifacts, score and intensity for each US parameter variation. In addition, the baseline and test US images are provided in Figure 2. A complete scheme containing all the different parameters tested is provided in Figures S1 and S2 (online only). The number of vertical artifacts in both phantoms is also listed in Table 1.

Vertical artifacts

Test recordings revealed that DR significantly changed the number of vertical artifacts, having a strong positive correlation with the mean number of artifacts ($R^2 = 0.916$, $p = 0.001$). A DR of 84 dB increased by one the mean number of vertical artifacts ($p = 0.04$), whereas a DR of 36 dB decreased the mean number of artifacts by two ($p = 0.002$) in four of five experts. An FA of 2 also increased the mean number of

Table 1
Numbers of vertical artifacts, experts' scores for optimal and suboptimal artifacts and intensity values for each tested parameter

	Test value (baseline value)	Vertical artifacts n (SD)	Optimal score (SD)	Intensity (dB)	Suboptimal score (SD)	Intensity (dB)
Baseline		4.4 (0.8)	11.6 (0.5)	−26	9.4 (1.7)	−24
Power, dB	−20 (vs. −10)	4.3 (0.9)	10.6 (1.1)	−50	9.9 (1.4)	−49
	−5 (vs. −10)	4.5 (1.2)	11.2 (1.1)	−23	9.5 (1.5)	−20
	0 (vs. −10)	4.6 (1.1)	11.8 (0.4)	−23	9.5 (1.2)	−20
Gain, %	85 (vs. 75)	4.1 (0.9)	11.2 (0.6)	−20	9.8 (1.6)	−17
	100 (vs. 75)	4.1 (0.8)	11.4 (0.8)	−12	9.0 (1,5)	−8
Frequency, MHz	6 (vs. 4)	4.2 (1.1)	11.6 (0.4)	−31	9.3 (1.4)	−27
	8 (vs. 4)	4.1 (0.9)	11.2 (0.8)	−34	9.1 (1.2)	−31
Artifact rejection	32 (vs. 0)	4.6 (0.8)	11.6 (0.6)	−28	9.3 (1.6)	−24
	64 (vs. 0)	4.2 (0.7)	11.2 (1.0)	−28	9.5 (1.8)	−23
Image enhancement	1 (vs. off)	4.8 (1.1)	11.1 (1.4)	−29	9.9 (1.9)	−24
	2 (vs. off)	4.8 (1.1)	11.6 (1.2)	−28	10.1 (2.0)	−24
	4 (vs. off)	4.7 (1.0)	10.8 (0.0)	−26	9.0 (1.7)	−21
Speckle reduction	Level 1 (vs. off)	4.8 (0.8)	11.4 (0.5)	−27	9.8 (1.8)	−22
	Level 5 (vs. off)	4.2 (0.7)	11.2 (0.8)	−27	9.0 (1.7)	−24
	Level 8 (vs. off)	4.0 (1.2)	11.1 (0.8)	−24	9.8 (1.7)	−22
Line density	Low (vs. medium)	4.6 (0.8)	11.4 (2.4)	−30	9.6 (2.1)	−27
	Standard (vs. medium)	4.6 (0.8)	11.0 (0.8)	−28	10.0 (1.9)	−23
	High (vs. medium)	4.6 (0.8)	11.0 (1.5)	−28	9.5 (1.8)	−23
Dynamic range, dB	36 (vs. 60)	3.1 (0.9)	11.2 (0.8)	−35	9.5 (1.7)	−29
	84 (vs. 60)	4.6 (0.6)	10.2 (1.9)	−24	9.8 (1.5)	−18
	102 (vs. 60)	4.9 (0.6)	10.9 (1.5)	−21	8.8 (1.6)	−16
Frame averaging	2 (vs. 0)	4.8 (0.3)	11.1 (0.8)	−29	10.1 (1.9)	−24
	4 (vs. 0)	4.3 (0.9)	11.5 (0.1)	−29	10.2 (2.1)	−24
	8 (vs. 0)	4.2 (1.2)	11.5 (0.2)	−31	10.3 (1.7)	−26

Data are expressed as the mean number of vertical artifacts, the mean score across the five experts and the standard deviation in parentheses.

vertical artifacts by one in four of five experts ($p = 0.03$). US settings such as power, image enhancement and speckle reduction increased by one in the number of vertical artifacts in at least two experts, but without statistical significance (Table 1).

There was no correlation between the number of vertical artifacts and their score. The optimal vertical artifact gathered with the baseline recordings scored 11.8 points (SD = 0.4) for phantom 1 and 11.2 points (SD = 0.7) for phantom 2. The suboptimal vertical artifact scored in baseline recordings 9.6 points (SD = 1.7) for phantom 1 and 9.2 points (SD = 1.7) for phantom 2. Regarding the influence of US parameters on the optimal vertical artifact score, a DR value of 84 dB (vs. 60 dB) decreased the mean score to 9.8 points (SD = 2.4) in phantom 1, whereas the low line density (vs. medium) decreased the mean score to 9.4 points (SD = 1.5) in phantom 2. US parameters did not significantly influence the suboptimal score in either phantom. In Figure 3, the mean vertical artifact score of both phantoms is given for optimal and suboptimal artifacts across the tested US parameters after baseline score normalization (*i.e.,* considered as 100%). The mean suboptimal vertical artifact score had an increased SD in test recordings compared with the optimal vertical artifact score.

The intensity values obtained in both phantoms were similar (Table 1). The intensity also correlated with neither the number of artifacts nor the score. Figure 4 illustrates the mean value of intensity and its variation with a 95% confidence interval of the US parameters. The DR significantly affected the intensity of vertical artifacts, increasing the intensity as its value increased ($R^2 = 0.976, p < 0.001$). The same could be seen with the increasing gain ($R^2 = 0.946, p = 0.003$) and power output ($R^2 = 0.683, p = 0.062$). On the other hand, an increase in frequency led to a significant decrease in the intensity of the vertical artifact ($R^2 = -0.956, p = 0.003$).

Discussion

In this work, we produced vertical artifacts using an *in vitro* model. We found that most LUS settings have a minor influence on their number and on the quality of "optimal" artifacts. The DR correlates positively with the mean number of vertical artifacts according to most experts on our panel. Regarding the quality of vertical artifacts, we created a descriptive score to evaluate subjectively the majority of vertical artifact features that are assessed in clinical practice. An optimal vertical artifact score was found to be negatively affected by high values of DR (>84 dB) and low values of line density, as indicated by a lack of contrast between the vertical artifact and the surrounding medium. Suboptimal artifacts had a high SD between expert scores, with no apparent trend attributable to any of the US parameters tested. The ROI intensity, as a measure of signal strength, correlated strongly and positively with DR, gain and power, and negatively with frequency. The influence of these US settings on laboratory vertical artifacts and the descriptive score of vertical artifact features may translate to the clinical practice.

Lung-mimicking phantoms

The phantoms created in this study represent a simplified model of the lung parenchyma. Physiological lung impedance depends on the volume fraction of air inside the alveoli. Therefore, vertical artifacts on the US examination may occur as a result of the reflected energy pulse from thickened lung interstitial spaces or an acoustic medium with higher impedance, such as blood or fluids, separated by ventilated spaces (*i.e.,* acoustic channels) [9]. Some reports have attempted to generate vertical artifacts by creating a bubble population in an enclosed space or aqueous sponge [9,24]. Demi et al. [10] confirmed that two different-sized microbubble populations exhibited more vertical artifacts and increased signal strength (*i.e.,* amplitude) as a function of microbubble size and probe frequency. Therefore, for reproducibility reasons, we created phantoms using methods already described as feasible [9,33,31]. We used a sponge with a mean diameter of 270 μm and an interspace of approximately 10 μm, corresponding to the known histological and normal alveolar sac [35]. Despite our efforts, proper mixing of the solution with gelatin and Metamucil was challenging to achieve. Five initial phantoms were discarded to avoid the recently recognized influence of "soft tissue noise" on vertical artifacts [11].

Vertical artifacts

Vertical artifacts were first described as ring-down artifacts [6]. Pathological vertical artifacts were described within the presence of
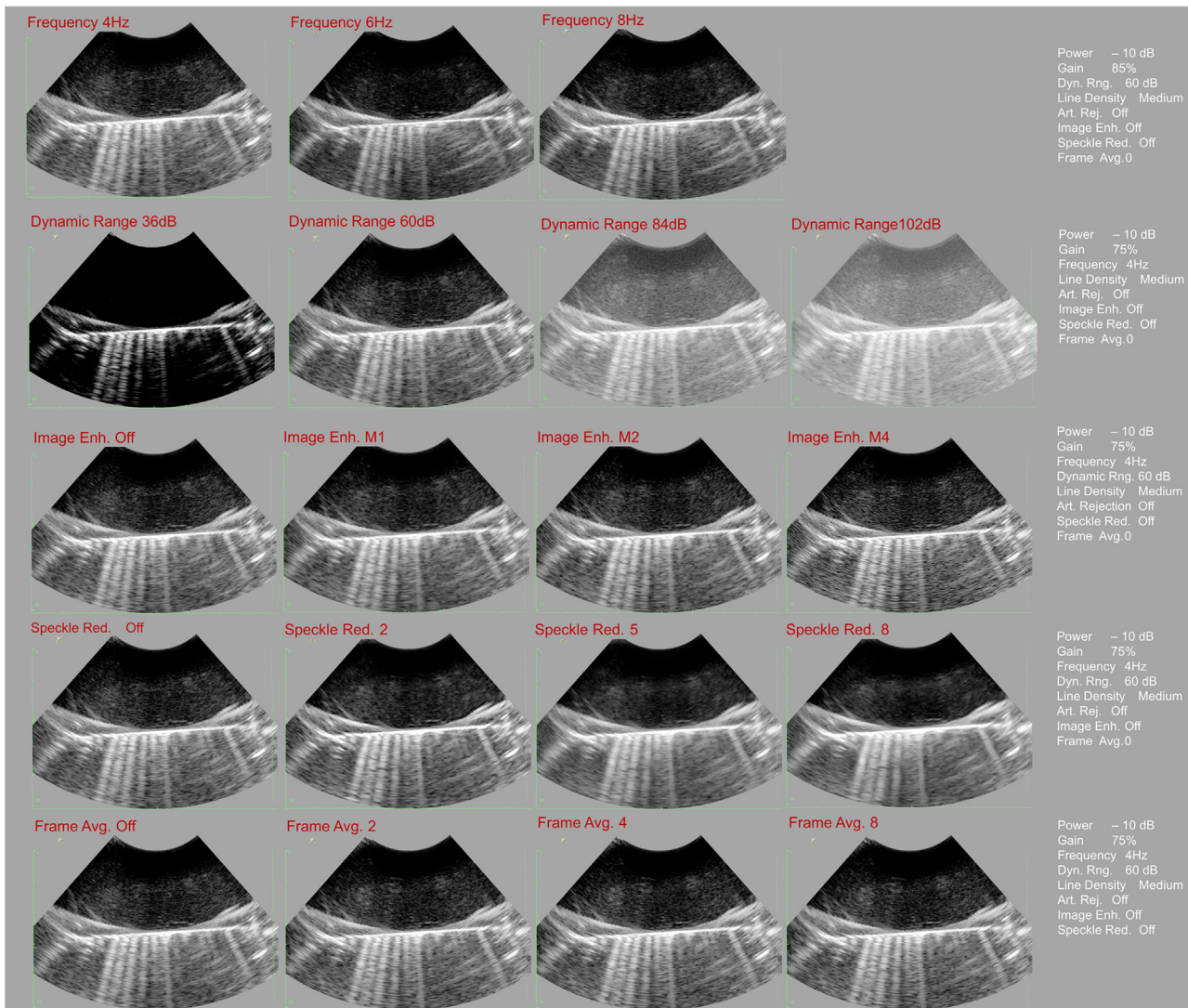
Figure 2. *In vitro* mode ultrasound images from phantom 2, from their lowest value (left) to the highest (right). Note the influence of the dynamic range in the appearance of the vertical artifacts.
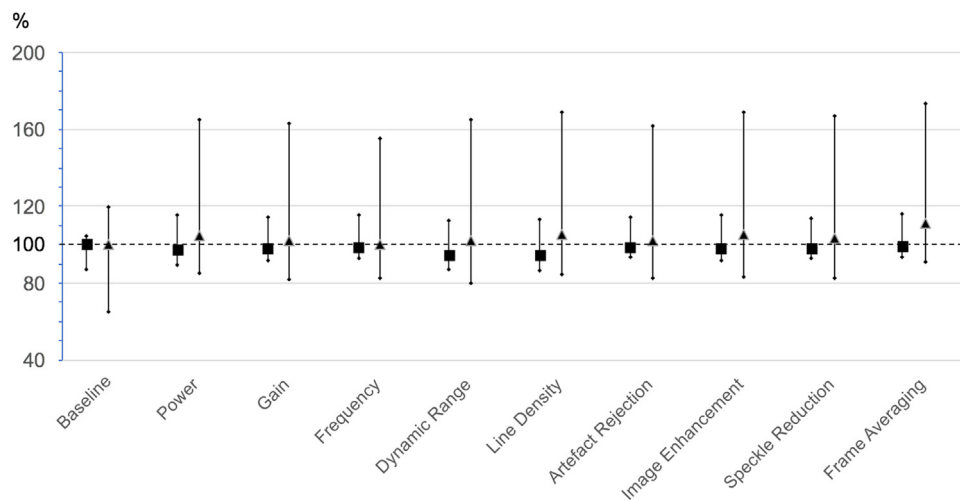

Figure 3. Mean score variation across the tested ultrasound parameters of optimal vertical artifacts (*squares*) and suboptimal vertical artifacts (*triangles*) after considering the score obtained in the baseline recording as 100%. Standard deviation (*lines*) of suboptimal vertical artifact mean score increases in comparison with that of the optimal score.
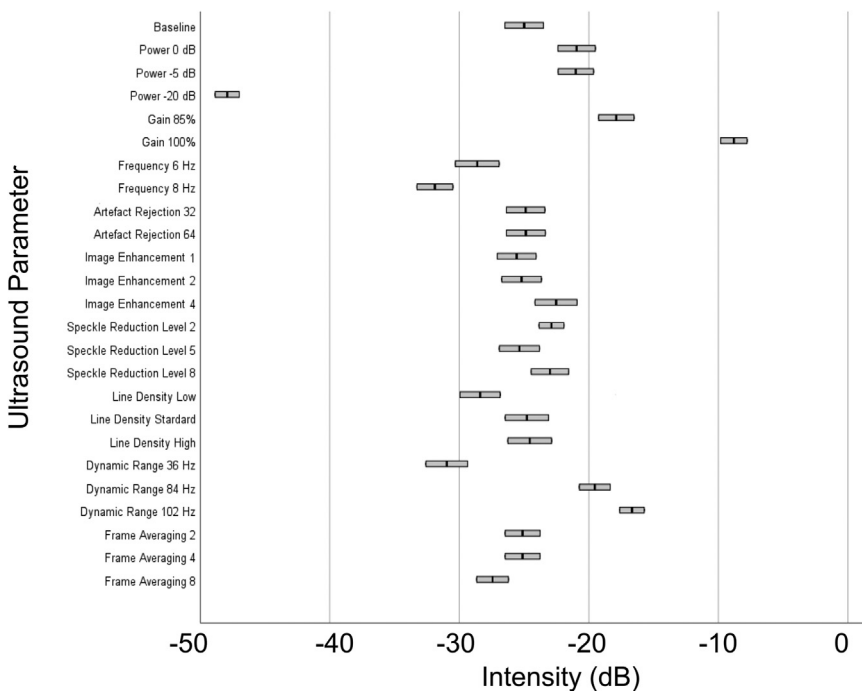
Figure 4. Signal intensity and 95% confidence interval of optimal and suboptimal vertical artifact signal intensity (dB) and 95% confidence interval for each ultrasound parameter. Note the decrease in intensity when increasing the probe frequency.

extravascular lung water and interstitial inflammation and during interstitial infiltrative processes [5,9,23]. Morphologically, the vertical artifacts are a linear artifact in the axis ("vertical") of the insonated US wave, starting from pleura with a "ring-down" appearance to the bottom of the screen, without fading [36]. Dietrich et al. [37] and recently Mathis et al. [34] alerted for the differences between lung comets and vertical artifacts because of their different origin mechanisms. Both originate from the pleural line and move with lung sliding; however, lung comets were believed to derive from a reverberation mechanism and fade out with increasing depth [34,36−38]. Conversely, a vertical artifact is composed of periodic and equal horizontal bands from the pleura to the bottom of the screen [5,9]. Simultaneously, others [9,11,12,26,39,40] investigated the physical origin of the vertical artifacts with *in vitro* and *in vivo* studies. To avoid confusion in nomenclature, the description "vertical artifacts" was introduced, and these were found to arise from the propagation of US waves and scattering reflection within an acoustic trap present on lung tissue with reduced aeration. This was done because the term *B-line*, as present throughout the literature on lung artifacts, was not descriptive enough. In turn, it may negatively influence the ability of the examiners to recognize these artifacts. In fact, vertical artifact morphology is dependent on both histopathology and US parameters [24]. Despite recent publications elucidating differences of such artifacts [13,23,34], only moderate to good intra-observer variability is achieved in recognizing vertical artifacts and in agreement in counting vertical artifacts between experts [29,41,42]. Matthias et al. [29] asked 14 reviewers from different backgrounds to quantify the number of vertical artifacts and assessed their quality after testing different US settings. This revealed a 95% confidence interval variation of up to 0.7 on a nominal scale of 0 to 5. For this purpose, recent international consensus [16,23,43] claimed the need to define the optimal imaging settings and understand their impact on US imaging.

The vertical artifacts observed in our study had the morphology of a ring down [34]. We selected US images with a wide range of vertical artifacts and tested different US parameters not tested in other reports. We then asked LUS experts to quantify their number. An FA of 2 and DR of 84 dB increased the mean number of vertical artifacts by one compared with US images without FA and with a DR of 60 dB. Such results may be supported by the biophysical origin of the vertical artifacts. After increasing the signal to noise ratio (*i.e.,* FA), the stronger scatter signals

were amplified, and some noise, caused by the sponge's water content surrounded by air, was removed, leading to more distinct vertical artifacts [6,9,38]. In addition, FA and DR resulted in an increased signal in the far field. As previously described, a reduced DR value (36 dB) removed up to two vertical artifacts [30,31].

In accordance with *in vivo* reports [11,28,38,44], our study indicated that most US settings do not significantly influence the number of vertical artifacts. However, our *in vitro* findings revealed that a DR of at least 60 dB is needed to avoid missing vertical artifacts. Furthermore, FA may help to enhance the far-field signal (*i.e.,* bottom screen). To our knowledge, this is the first study reporting a small effect of these US parameters. Despite the already known influence of center frequency on morphology of vertical artifacts [12,26,31,39,40] in our study, the frequency range between 4 and 8 MHz does not affect the mean counting of vertical artifacts by US experts. Such subjective analysis may be prone to erroneous conclusions, but it still translates human eye capacity to identify vertical artifacts.

Regarding the influence of US parameters on vertical artifact morphology, we asked LUS experts to score each vertical artifact. The artifacts with the highest and lowest average values, which the experts considered to be vertical artifacts, were designated as "optimal" and "suboptimal," respectively. We attempted to include in the score the major visual aspects of the vertical artifacts (*i.e.,* pleura, length and strength of the signal, boundary contrast). This contrasts with other reports, which have used more qualitative scales to visually rate vertical artifact morphology as "better" than the baseline measurement [30]. In addition, despite an international effort to standardize and use quantitative methods for vertical artifact evaluation [23], the clinical utility of enhancing and identifying every vertical artifact remains to be studied. In other words, the vertical artifacts described with ring-down appearance still remain the ones that correlate with interstitial pulmonary diseases, lung water volume and pulmonary artery pressure [8,14,17−19].

A low line density blurred the horizontal and vertical transitions of the vertical artifacts, which may obviate the ring-down artifact and increase its width. Despite the need to validate our study results *in vivo*, a line density value of zero may blur a vertical artifact. On other hand, an increase in DR (>84 dB) decreased the expert's mean score, in accordance with *in vivo* experiments [38].

As per definition, the suboptimal vertical artifact scored significantly lower than the optimal one. Although some of the tested US parameters

positively influenced the mean score of the suboptimal artifacts, a high variation in score between experts precluded further interpretation. Suboptimal artifacts appeared as small vertical artifacts resembling lung comets and seemed more likely to change after altering the settings of the US device. However, the relevance of poorly defined lung artifacts and their optimization remains unknown in clinical practice.

According to recent findings [24,40] vertical artifacts may be enhanced by some US parameters depending on pulmonary pathology. Some vertical artifacts resemble anteriorly named Z-lines [37], and therefore, their presence does not necessarily imply an increased alveoli water volume [44]. However, such artifacts do not exhibit classic features of pulmonary edema. In fact, the clinical utility of such vertical artifacts remains to be studied and standardized [23].

Intensity

The total intensity of optimal and suboptimal vertical artifacts was extracted from US imaging as a measure of signal strength. Mento et al. [45] developed a method to perform US imaging spectroscopy from the vertical artifacts of patients with pulmonary fibrosis. They reported that the mean total intensity was higher in non-fibrotic patients (0.64 dB) than in fibrotic patients (-4.76 dB). After extracting the frequency and total intensity from the vertical artifacts, they detected fibrotic patients in a cohort of 26 patients with a sensitivity and specificity of 92% and 92%, respectively. In our study, we used the same method to extract the total intensity of vertical artifacts. The influence of US parameters on intensity did not correlate with the mean number of vertical artifacts or score, although increasing frequency and image averaging led to a decrease in signal intensity. Shorter wavelengths (*i.e.,* increased probe frequency) may decrease the amplitude of the reflected waves depending on the acoustic channel size [12,31,39,46], whereas the average signal amplitude may be lower than the original reflected wave signal. Moreover, US gain is based on the coherent sum of identical waveforms [47]. When increasing the gain, the signal amplitude within the selected ROI also increases as signal intensity. In fact, similar behavior occurs when power (also in decibels) and DR increase.

There are no other studies focusing on vertical artifact image signal intensity data from *in vitro* models or healthy volunteers. The "optimal" vertical artifact signal intensity may provide useful information in developing algorithms for automatic artifact detection. In fact, such algorithms could increase the reproducibility of the automatic counting of the vertical artifacts and, hence, facilitate comparison studies, especially in the case where different equipment and settings are used [48]. In addition, contributions to this field are needed as stated in the newly international consensus [23].

Limitations

In clinical practice, the air volume inside the alveoli changes across diseases. *In vitro* and experimental phantoms represent only a simplified model of the lung parenchyma. Furthermore, such a static model does not accurately represent pathological changes in a complex moving tissue such as the lung. Aside from the influence of frequency, focal point, dynamic range and incidence angle on vertical artifacts, the influence of other US parameters has not been tested [16,30,32,33]. Our model was immobile to ensure that the same volume of interest was evaluated after changing US settings. In addition, our model had a depth of only 6 cm, making it less vulnerable to the influence of US settings on vertical artifacts, mainly those in the far field. The observed depth of the vertical artifacts in our study was smaller than those commonly reported in the literature [4,8,12]. The reason for this might be related to the fact that the phantom might not accurately characterize the tissue, as discussed previously. However, after review of the recorded US images, the majority of "optimal" vertical artifacts scored 3 points in length (*i.e.,* longer than 20 mm).

Additionally, the averaged intraclass correlation coefficient for the number of vertical artifacts was relatively low (*i.e.,* 0.694). Despite being within the reported range in the literature [29,42], our results may be influenced by the wide range of experience in LUS (from 3 to 10 y) within the EchoCrit Group. Although we created the vertical artifact score using current literature and expert opinion, it may not have been sensitive enough to capture all the features of the vertical artifacts, potentially leading to a lack of significant changes in the scores obtained. Such subjective analysis was based on the features of the vertical artifacts *in vitro* and was qualitative and dependent on LUS experts. Therefore, our results might require further validation.

Another limitation was the equipment and software used, which did not allow evaluation of other US parameters, some of which have been reported to affect vertical artifacts, such as harmonics [46]. In this study, a pediatric convex probe was used, and other types of probes have also been reported to affect vertical artifacts [30]. (When a convex probe is used, the lateral size of a vertical artifact naturally increases far from the pleural plane because the US system's signal/image processing algorithms convert signals into a 2-D image.) In addition, the lateral size of an artifact (produced by a convex probe) at the screen's end depends on the image's depth [31]. In contrast, a consistently narrow artifact is common when using a linear probe [17].

Conclusion

In this study, we evaluated the influence of US imaging parameters on vertical artifacts. To this end, we created a descriptive score based on the morphology of these artifacts. The vertical artifact with the highest score was termed "optimal," whereas that with the lowest score was termed "suboptimal." Our results indicate that variation of most of the US parameters does not significantly affect the number and scoring of optimal vertical artifacts. DR and FA were the only parameters that significantly affected the number of vertical artifacts. Even though artifact intensity correlates strongly with power, gain, DR and frequency, the quality of an optimal vertical artifact was not altered. Future studies should validate the utility of the vertical artifact score and signal intensity evaluation.

Conflict of interest

The authors declare no competing interests. This study follows the European Code of Conduct for Research Integrity and adheres to all good investigative practices.

Data availability statement

The images dataset used during the present study are shown in the supplementary material. The numerical data are available from the corresponding author on request.

Supplementary materials

Supplementary material associated with this article can be found in the online version at doi:10.1016/j.ultrasmedbio.2023.03.018.

References

[1] Ñamendys-Silva SA, Garrido-Aguirre E, Romero-González JP, Mena-Arceo RG. Rojo Del Moral O, González-Chon O. Pulmonary ultrasound: a new era in critical care medicine. Ultrasound Q 2018;34:219−25. doi: 10.1097/RUQ.0000000000000357.

[2] Zieleskiewicz L, Markarian T, Lopez A, Taguet C, Mohammedi N, Boucekine M, et al. AZUREA Network. Comparative study of lung ultrasound and chest computed tomography scan in the assessment of severity of confirmed COVID-19 pneumonia. Intensive Care Med 2020;46:1707−13. doi: 10.1007/s00134-020-06186-0.

[3] Marini TJ, Rubens DJ, Zhao YT, Weis J, O'Connor TP, Novak WH, et al. Lung ultrasound: the essentials. Radiol Cardiothorac Imaging 2021;3:e200564.

[4] Leote J, Judas T, Broa AL, Lopes M, Abecasis F, Pintassilgo I, et al. Time course of lung ultrasound findings in patients with COVID-19 pneumonia and cardiac dysfunction. Ultrasound J 2022;14:28. doi: 10.1186/s13089-022-00278-2.

[5] Volpicelli G, Elbarbary M, Blaivas M, Lichtenstein DA, Mathis G, Kirkpatrick AW, et al. International Liaison Committee on Lung Ultrasound (ILC-LUS) for International Consensus Conference on Lung Ultrasound (ICC-LUS): international evidence-based recommendations for point-of-care lung ultrasound. Intensive Care Med 2012;38:577−91.

[6] Avruch L, Cooperberg PL. The ring-down artifact. J Ultrasound Med 1985;4:21−8.

[7] Lichtenstein D, Mézière G, Biderman P, Gepner A, Barré O. The comet-tail artifact: an ultrasound sign of alveolar−interstitial syndrome. Am J Respir Crit Care Med 1997;156:1640−6. doi: 10.1164/ajrccm.156.5.96-07096.

[8] Volpicelli G, Mussa A, Garofalo G, Cardinale L, Casoli G, Perotto F, et al. Bedside lung ultrasound in the assessment of alveolar−interstitial syndrome. Am J Emerg Med 2006;24:689−96. doi: 10.1016/j.ajem.2006.02.013.

[9] Soldati G, Demi M, Inchingolo R, Smargiassi A, Demi L. On the Physical basis of pulmonary sonographic interstitial syndrome. J Ultrasound Med 2016;35:2075−86.

[10] Demi L, van Hoeve W, van Sloun RJG, Soldati G, Demi M. Determination of a potential quantitative measure of the state of the lung using lung ultrasound spectroscopy. Sci Rep 2017;7:12746. doi: 10.1038/s41598-017-13078-9.

[11] Demi L, Egan T, Muller M. Lung ultrasound imaging, a technical review. Appl Sci 2020;10:462. doi: 10.3390/app10020462.

[12] Demi L, Demi M, Prediletto R, Soldati G. Real-time multi-frequency ultrasound imaging for quantitative lung ultrasound—first clinical results. J Acoust Soc Am 2020;148:998.

[13] Mohanty K, Blackwell J, Egan T, Muller M. Characterization of the lung parenchyma using ultrasound multiple scattering. Ultrasound Med Biol 2017;43:993−1003.

[14] Volpicelli G, Caramello V, Cardinale L, Mussa A, Bar F, Frascisco MF. Detection of sonographic B-lines in patients with normal lung or radiographic alveolar consolidation. Med Sci Monit 2008;14:CR122−8.

[15] Sferrazza Papa GF, Pellegrino GM, Volpicelli G, Sferrazza Papa S, Di Marco F, Mondoni M, et al. Lung ultrasound B lines: etiologies and evolution with age. Respiration 2017;94:313−4. doi: 10.1159/000479034.

[16] Laursen CB, Clive A, Hallifax R, Pietersen PI, Asciak R, Davidsen JR, et al. European Respiratory Society statement on thoracic ultrasound. Eur Respir J 2021;57:2001519. doi: 10.1183/13993003.01519-2020.

[17] Mojoli F, Bouhemad B, Mongodi S, Lichtenstein D. Lung ultrasound for critically ill patients. Am J Respir Crit Care Med 2019;199:701−14. doi: 10.1164/rccm.201802-0236CI.

[18] Lichtenstein DA, Mezière GA, Lagoueyte JF, Biderman P, Goldstein I, Gepner A. A-lines and B-lines: lung ultrasound as a bedside tool for predicting pulmonary artery occlusion pressure in the critically ill. Chest 2009;136:1014−20. doi: 10.1378/chest.09-0001.

[19] Mayr U, Lukas M, Habenicht L, Wiessner J, Heilmaier M, Ulrich J, et al. B-lines scores derived from lung ultrasound provide accurate prediction of extravascular lung water index: an observational study in critically ill patients. J Intensive Care Med 2022;37:21−31.

[20] Russell FM, Ferre R, Ehrman RR, Noble V, Gargani L, Collins SP, et al. What are the minimum requirements to establish proficiency in lung ultrasound raining for quantifying B-lines? ESC Heart Fail 2020;7:2941−7. doi: 10.1002/ehf2.12907.

[21] Kameda T, Kamiyama N, Kobayashi H, Kanayama Y, Taniguchi N. Ultrasonic B-line-like artifacts generated with simple experimental models provide clues to solve key issues in B-lines. Ultrasound Med Biol 2019;45:1617−26. doi: 10.1016/j.ultrasmedbio.2019.03.003.

[22] Hasan AA, Makhlouf HA. B-lines: Transthoracic chest ultrasound signs useful in assessment of interstitial lung diseases. Ann Thorac Med 2014;9:99−103.

[23] Demi L, Wolfram F, Klersy C, De Silvestri A, Ferretti VV, Muller M, et al. New international guidelines and consensus on the use of lung ultrasound. J Ultrasound Med 2023;42:309−44. doi: 10.1002/jum.16088.

[24] Soldati G, Smargiassi A, Demi L, Inchingolo R. Artifactual lung ultrasonography: it is a matter of traps, order, and disorder. Appl Sci 2020;10:1570.

[25] Kameda T, Kamiyama N, Taniguchi N. The mechanisms underlying vertical artifacts in lung ultrasound and their proper utilization for the evaluation of cardiogenic pulmonary edema. Diagnostics (Basel) 2022;12:252. doi: 10.3390/diagnostics12020252.

[26] Buda N, Skoczylas A, Demi M, Wojteczek A, Cylwik J, Soldati G. Clinical impact of vertical artifacts changing with frequency in lung ultrasound. Diagnostics (Basel) 2021;11:401. doi: 10.3390/diagnostics11030401.

[27] Bobillo-Perez S, Girona-Alarcon M, Rodriguez-Fanjul J, Jordan I, Balaguer Gargallo M. Lung ultrasound in children: what does it give us? Paediatr Respir Rev 2020;36:136−41.

[28] Mento F, Demi L. On the influence of imaging parameters on lung ultrasound B-line artifacts, in vitro study. J Acoust Soc Am 2020;148:975−83. doi: 10.1121/10.0001797.

[29] Matthias I, Panebianco NL, Maltenfort MG, Dean AJ, Baston C. Effect of machine settings on ultrasound assessment of B-lines. J Ultrasound Med 2021;40:2039−46.

[30] Schmickl CN, Menon AA, Dhokarh R, Seth B, Schembri F. Optimizing B-lines on lung ultrasound: an in-vitro to in-vivo pilot study with clinical implications. J Clin Monit Comput 2020;34:277−84. doi: 10.1007/s10877-019-00321-z.

[31] Mento F, Demi L. Dependence of lung ultrasound vertical artifacts on frequency, bandwidth, focus and angle of incidence: an in vitro study. J Acoust Soc Am 2021;150:4075.

[32] Lo MD, Ackley SH, Solari P. Homemade ultrasound phantom for teaching identification of superficial soft tissue abscess. Emerg Med J 2012;29:738−41.

[33] Blüthgen C, Sanabria S, Frauenfelder T, Klingmüller V, Rominger M. Economical sponge phantom for teaching, understanding, and researching A- and B-line reverberation artifacts in lung ultrasound. J Ultrasound Med 2017;36:2133−42. doi: 10.1002/jum.14266.

[34] Mathis G, Horn R, Morf S, Prosch H, Rovida S, Soldati G, et al. WFUMB position paper on reverberation artifacts in lung ultrasound: B-lines or comet-tails? Med Ultrason 2021;23:70−3. doi: 10.11152/mu-2944.

[35] Sagar KB, Rhyne TL, Myers GS, Lees RS. Characterization of normal and abnormal pulmonary surface by reflected ultrasound. Chest 1978;74:29−33. doi: 10.1378/chest.74.1.29.

[36] Yue Lee FC, Jenssen C, Dietrich CF. A common misunderstanding in lung ultrasound: the comet tail artefact. Med Ultrason 2018;20:379−84. doi: 10.11152/mu-1573.

[37] Dietrich CF, Mathis G, Blaivas M, Volpicelli G, Seibel A, Wastl D, et al. Lung B-line artifacts and their use. J Thorac Dis 2016;8:1356−65.

[38] Dietrich CF, Mathis G, Blaivas M, Volpicelli G, Seibel A, Atkinson NS, et al. Lung artifacts and their use. Med Ultrason 2016;18:488−99.

[39] Peschiera E, Mento F, Demi L. Numerical study on lung ultrasound B-line formation as a function of imaging frequency and alveolar geometries. J Acoust Soc Am 2021;149:2304.

[40] Demi M, Prediletto R, Soldati G, Demi L. Physical mechanisms providing clinical information from ultrasound lung images: hypotheses and early confirmations. IEEE Trans Ultrason Ferroelectr Freq Control 2020;67:612−23. doi: 10.1109/TUFFC.2019.2949597.

[41] Anderson KL, Fields JM, Panebianco NL, Jenq KY, Marin J, Dean AJ. Inter-rater reliability of quantifying multiple B-lines using multiple counting methods. J Ultrasound Med 2013;32:115−20. doi: 10.7863/jum.2013.32.1.115.

[42] Gullett J, Donnelly JP, Sinert R, Hosek B, Fuller D, Hill H, et al. Interobserver agreement in the evaluation of B-lines using bedside ultrasound. J Crit Care 2015;30:1395−9.

[43] Stanton AE, Edey A, Evison M, Forrest I, Hippolyte S, Kastelik J, et al. British Thoracic Society training standards for thoracic ultrasound (TUS). BMJ Open Respir Res 2020;7:e000552. doi: 10.1136/bmjresp-2019-000552.

[44] Lichtenstein D. Novel approaches to ultrasonography of the lung and pleural space: where are we now? Breathe (Sheff) 2017;13:100−11. doi: 10.1183/20734735.004717.

[45] Mento F, Soldati G, Prediletto R, Demi M, Demi L. Quantitative lung ultrasound spectroscopy applied to the diagnosis of pulmonary fibrosis: the first clinical study. IEEE Trans Ultrason Ferroelectr Freq Control 2020;67:2265−73.

[46] Volpicelli G, Gargani L, Perlini S, Spinelli S, Barbieri G, Lanotte A, et al. on behalf of the International Multicenter Study Group on LUS in COVID-19. Lung ultrasound for the early diagnosis of COVID-19 pneumonia: an international multicenter study. Intensive Care Med 2021;47:444−54. doi: 10.1007/s00134-021-06373-7.

[47] Contreras Ortiz SH, Chiu T, Fox MD. Ultrasound image enhancement: a review. Biomed Signal Process Control 2012;7:419−28. doi: 10.1016/j.bspc.2012.02.002.

[48] Quarato CMI, Venuti M, Sperandeo M. The artificial count of artifacts for thoracic ultrasound: what is the clinical usefulness? J Clin Monit Comput 2020;34:1379−81.